Geological, petrographical and petrological characteristics of ultramafic-mafic xenoliths in Kurose and Takashima, northern Kyushu, southwestern Japan

Shoji ARAI[1], Natsue ABE[2], Hisatoshi HIRAI[3] and Yohei SHIMIZU[1]

1 Department of Earth Sciences, Kanazawa University, Kanazawa 920-1192, Japan

2 GEMOC, Department of Earth & Planetary Sciences, Macquarie University, Sydney, NSW 2109, Australia

3 National Institute of Advanced Industrial Science and Technology (AIST) Kyushu, Tosu, Saga 841-0052, Japan

Abstract : Characteristics of ultramafic xenoliths are quite different between Kurose and Takashima, which are only 30 km apart each other, in northern Kyushu, the Southwestern Japan arc. The host rock is slightly nepheline-normative alkaline basalt for both localities, and the age is 1.1 Ma for Kurose and is 3.0 Ma for Takashima. Mantle lherzolite/harzburgite is predominant over Group I rocks (dunite and pyroxenites), and Group II xenoliths and related black pyroxene megacrysts are almost absent in Kurose. Mantle peridotite is almost absent and, instead, Group I rocks are prominent both in volume and in lithological variation, from dunite to pyroxenites, in Takashima. Group II xenoliths and related megacrysts are abundant in Takashima basalt. Group I rocks of Takashima were penetrated by a silica-oversaturated melt to produce Group III pyroxenites. These rocks were finally invaded by Group II rocks.

This contrast between the two xenolith suites indicates a strong lateral heterogeneity of the uppermost mantle in terms of extent both of Group I dunite-pyroxenites and of Group II rocks, in the Southwest Japan arc, especially in northern Kyushu area. Group I rocks are basically cumulates from some island arc magma(s), and the dunite especially is a possible reaction product between peridotite and arc magma. Group II rocks are deep-seated cumulates from the alkali basalts that had preceded the host basalt in the same area or the same volcano cluster. The alkali basaltic melts involved in the Group II formation gave a strong chemical effect (metasomatism) on surrounding Group I rocks. This complicated and heterogeneous upper mantle has been accomplished at the rim of the Western Pacific where magmatism of arc and back arc has been active.

1. Introduction

Ultramafic and related xenoliths in magmas give us unrivaled insights into petrological constitution of deep parts of island arcs or continents that are otherwise inaccessible. The Japanese island arcs especially provide us with ultramafic xenoliths of possible mantle wedge origin (Takahashi, 1978 ; Aoki, 1987). In contrast to this, almost all localities of ultramafic xenoliths of the world are located on continental rift zones and oceanic hot spots (Nixon, 1987).

In the southwest Japan arc there have been many localities documented where we can obtain various ultramafic xenoliths from Cenozoic alkali basalts and related volcanics (e.g., Takamura, 1973 ; Takahashi, 1978 ; Arai et al., 2000) (Fig. 1). Takashima and Kurose among them are located, being only 30 km apart each other, in the northern Kyushu area, and provide quite different xenolith suites from one another. This will give us an excellent insight into the upper mantle constitution, especially its petrological heterogeneity, beneath the Japan island arc. Ultramafic xenoliths of Kurose and Takashima were described and briefly discussed by Kobayashi and Arai (1981), Arai and Kobayashi (1981), Arai and Hirai (1983) and Arai et al. (2000).

In contrast to the Southwest Japan arc, there are only two volcanoes that provide us peridotite xenoliths, Megata volcano (Kuno, 1967 ; Aoki and Shiba, 1973 ; Aoki and Prinz, 1974 ; Takahashi, 1978, 1986) of the Oga Peninsula, and Oshima-Oshima volcano (Yamamoto, 1984 ; Ninomiya and Arai, 1992) in the Sea of Japan off Hokkaido. The host

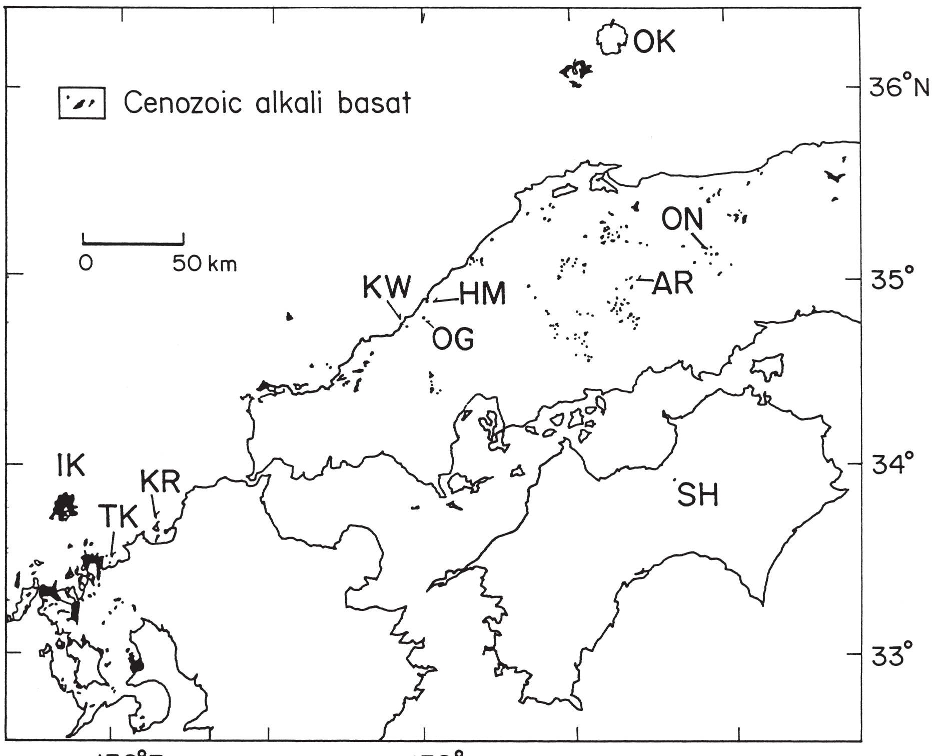

Fig. 1. Distribution of Cenozoic alkali basalts in the Southwest Japan arc (modified from Takamura, 1973). Note that they often make clusters. Main localities of deep-seated xenoliths are indicated : OK, Oki-Dogo ; ON, On-yama ; AR, Aratoyama ; HM, Hamada ; OG, Noyamadake ; KW, Kawashimo ; SH, Shingu ; IK, Iki ; KR, Kurose ; and TK, Takashima.

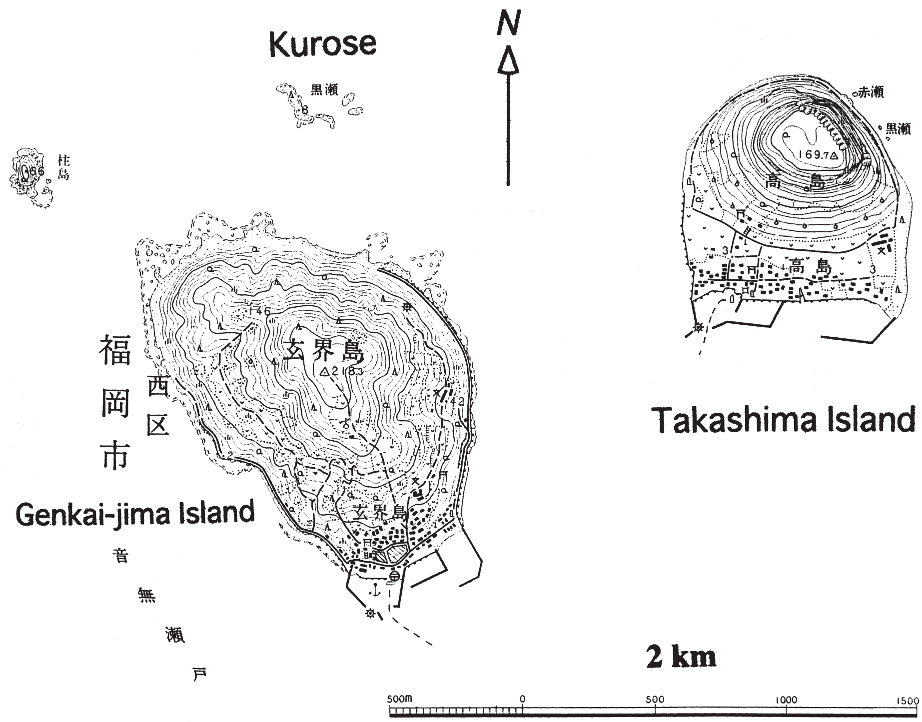

Fig. 2. Topographical maps of Kurose and Takashima. Made from 1 : 25,000 topographical maps of " Karatsu" and "Genkai-jima" issued by the Geographical Survey Institute, Japan.

magmas for the two xenolith suites are of island-arc type, high-alumina basalt and calc-alkaline andesite to dacite for Megata volcano (Katsui et al. 1979 ; Aoki and Fujimaki, 1982 ; Sakuyama and Koyaguchi, 1984), and calc-alkaline andesite for Oshima-Oshima volcano (Katsui et al., 1979).

2. Geological background

There are many localities of Cenozoic alkali basalts and related volcanics that produce deep-seated rocks as xenoliths (Fig. 1). They usually make volcano clusters, which have distinct characteristics of age and chemistry of magmas (Uto, 1990 ; Iwamori, 1991). The oldest of them is Shingu alkali basalt (lamprophyre) dikes on Shikoku Island, of which age is 17.7 Ma (Uto et al., 1987) (Fig. 1). Kurose and Takashima belong to the youngest ones of them. Takashima alkali basalt belongs to the Higashi-Matsuura volcano cluster, and Kurose alkali basalt is isolated from other clusters (Fig. 1).

2.1 Kurose

Kurose (= Black Rock in Japanese) is a reef-like rock of alkali basalt off Genkai-jima Island at the mouth of Hakata Bay (Figs. 1 and 2). The Genkai-jima Island is composed of

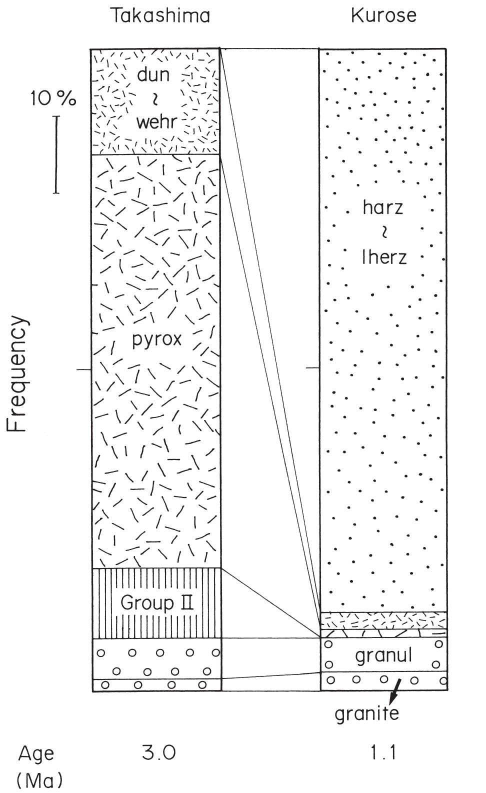

Fig. 3. Frequency diagrams of xenolith rock species and K-Ar ages of host basalts from Kurose and Takashima (eastern coast). Ages from Uto et al. (1993) and Nakamura et al. (1986). Note the difference between the two localities. harz, harzburgite ; lherz, lherzolite ; dun, dunite ; wehr, wehrlite ; pyrox, pyroxenites ; granul, granulite.

Cretaceous granite, through which the alkali basalt erupted at 1.1 Ma (Uto et al., 1993). No pyroclastics are found around Kurose. The alkali basalt is slightly porous and light gray in color, frequently showing flow foliations on the outcrop. Pillow-like structures are occasionally observed. The Kurose alkali basalt is abundant in xenoliths, which are up to 30 cm across, angular to rounded in shape, and are various from feldspathic (granulite) to peridotitic via websterites. The most important is the almost absence of black pyroxene megacrysts and related pyroxenites of Group II in the sense of Frey and Prinz (1978) (Fig. 3). Loosely packed black pyroxenites of Group II are rarely found.

2.2 Takashima

Takashima (=Tall Island in Japanese) is a kind of mesa of granodiorite capped by alkali basalt of 3.0 Ma in age (Nakamura et al., 1986) in Karatsu Bay (Figs. 1 and 2). The cliff of alkali basalt is not accessible but we can observe boulders of various volcanics on the shore of the islet of Takashima. Alkali basalt lavas show various lithologies, from fine-grained black one to coarser-grained grayish one. It is sometimes highly plagioclase-phyric. Vent-opening pyroclastics underlie the lava flows, and directly cover the basement of granodiorite. Xenoliths up to 50 cm across and megacrysts up to 5 cm across are abundantly included in all kinds of volcanics. Peridotite xenoliths have been selectively eroded to be concave and, are unfortunately difficult to sample from hard alkali basalt boulders, which are frequently rounded by wave action.

Peridotites and pyroxenites are predominant over feldspathic rocks ; granulite (rare), gabbros and basement granodiorite, which is considerably digested to be have small druses inside and glass-rich halo around xenoliths. Variations of frequency of xenolith species are observed depending on the difference of host rock types (lithologies) (Fig. 4). The pyroclasitics are basically composed of comminuted granodioritic materials and essential fragments with small xenoliths and megacrysts (Fig. 5). Gabbro xenoliths are more abundant

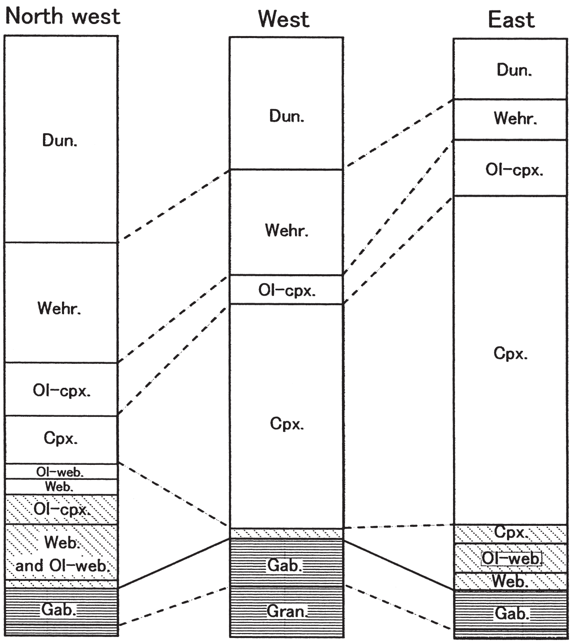

Fig. 4. Frequency diagrams of xenolith rock species in alkali basaltic lavas at three localities from Takashima. Dun, dunite ; Wehr, wehrlite ; Ol-cpx, olivine clinopyroxenite ; Cpx, clinopyroxenite ; Web, websterite ; Ol-web, olivine websterite ; Gab, gabbro and mafic granulite ; Gran, granodiorite. Group II rocks are obliquely ruled, and crustal rocks are horizontally ruled.

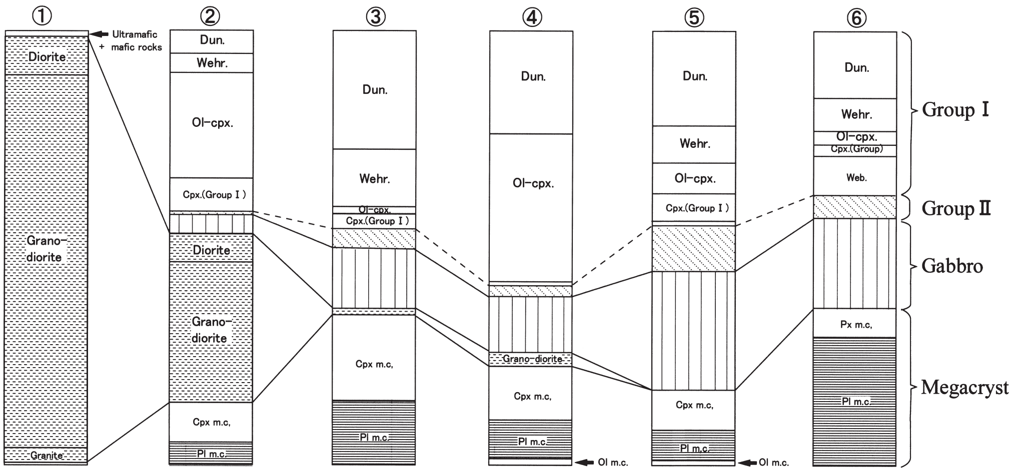

Fig. 5. Frequency diagrams of xenolith rock species in various volcanics of Takashima. 1, lapilli stone ; 2, ill-sorted tuff breccia with essential blocks and bombs ; 3, essential blocks and bombs of 2 ; 4, lapilli tuff ; 5, weakly welded tuff ; 6, plagioclase-rich lava.

relative to ultramafic ones in pyroclastics than in lavas (Figs. 4 and 5). This possibly implies a kind of fractionation of xenolith species in alkali basalt magmatic column within a conduit before eruption (Hirai, 1983).

Megacrysts are dominated by pitch-black clinopyroxene and orthopyroxene with subordinate plagioclase (andesine) (Kuno, 1964). Orthopyroxene megacrysts are always surrounded by leucocratic reaction rim.

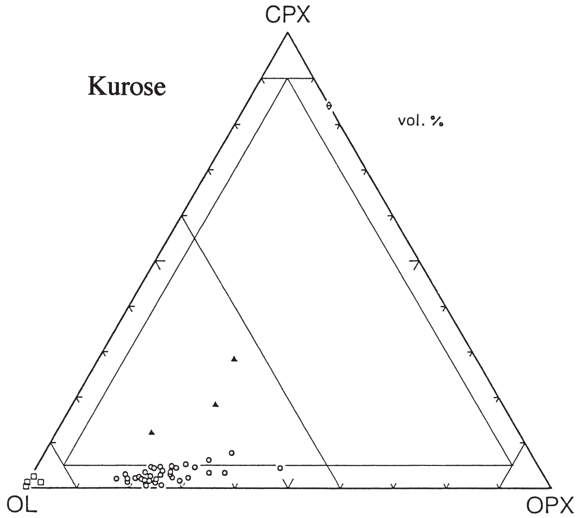

Fig. 6. Modal amounts of olivine and pyroxenes in ultramafic xenoliths from Kurose. Open square, dunite ; open circle, harzburgite/lherzolite ; closed triangle, pyroxene-rich lherzolite ; diamond, websterite.

3. Petrography

Typical mantle peridotite xenoliths from the Japan island arcs are shown in Plate I for comparison. The textural variety is noteworthy.

3.1 Kurose

The Kurose alkali basalt is vesicular, and has phenocrysts or microphenocrysts of olivine (< 0.5 mm) and titanaugite. Groundmass is composed of euhedral olivine, titanaugite, plagioclase, magnetite, alkali feldspar (subhedral to anhedral) and zeolites. Xenocrysts of olivine and orthopyroxene, derived from disaggregated peridotite xenoliths, are also found. The basalt is moderately silica-undersaturated and has about 6 % of normative nepheline (Table 1). It is higher in Na_2O amount relative to K_2O than an averaged Cenozoic alkali basalt in the Southwest Japan arc (Takamura, 1973), leading to having high normative Ab and low normative Or contents.

More than 1,700 xenoliths were examined on the outcrop for the size and rock species to determine the frequency (volume ratio) of the rock species in the Kurose xenolith suite (Fig. 3). Harzburgite and lherzolite are predominant over dunite-wehrlite, pyroxenites (mostly websterite) and mafic granulites (Fig. 3). The mantle peridotite is moderately foliated and is relatively fine-grained (1 to 2 mm across) (Plate II). It has typically equigranular to porphyroclastic textures (Plate II) : olivine has straight grain boundaries that have nice triple junctions. Clinopyroxene is up to 8 vol. % and cpx/(opx + cpx) volume ratio is around 0.05, meaning that the peridotite is around the boundary between lherzolite and harzburgite (Arai et al., 2000 ; Fig. 6). Olivine and orthopyroxene commonly show kink bands and wavy extinction, respectively. Orthopyroxene has only thin exsolution lamellae of clinopyroxene. Finer-grained pyroxene-rich lherzolite is sometimes found, and its spinel is light greenish brown indicating its fertile aluminous character (Plate II). Websterites are

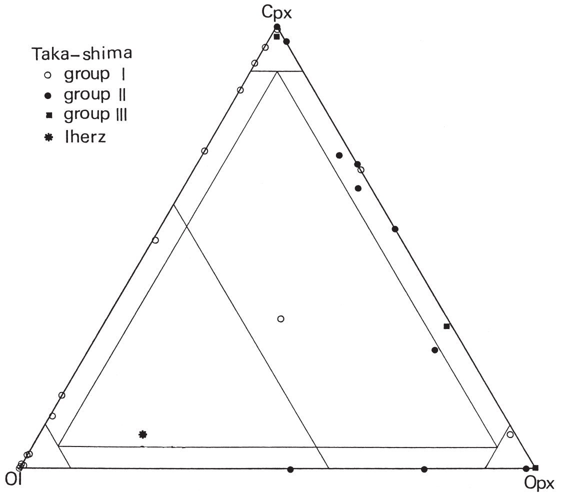

Fig. 7. Modal amounts of olivine and pyroxenes of Takashima xenoliths. Note their wide lithological variation.

usually free from olivine, and contain green spinel (Plate II). Granulite is composed of plagioclase, clinopyroxene, orthopyroxene and green spinel (Plate II), and is apparently continuous in mode to websterite with a decrease of plagioclase and an increase of green spinel. Clinopyroxene is slightly dominant over orthopyroxene in volume in these rocks. It is noteworthy that olivine does not coexist with plagioclase in all Kurose xenoliths.

The Group II xenoliths are mostly cpx-rich websterite (Plate II), composed of irregular-shaped grains up to 2 mm across of clinopyroxene and orthopyroxene. Pyroxenes have exsolution lamellae with various thickness. Clinopyroxene occasionally have trace amounts of kaersutite and rhoenite blebs up to 50 microns, occasionally associated with orthopyroxene lamellae.

3.2 Takashima

The host rock is alkali basalt (Table 1), containing phenocrysts of olivine, clinopyroxene and plagioclase, and the groundmass of plagioclase, olivine, clinopyroxene, magnetite and zeolites. Druses are filled with clays, zeolites and calcite (Kobayashi and Arai, 1981).

Almost all xenoliths can be divided into two groups, I and II, in the sense of Frey and Prinz (1978). Group I xenoliths have green clinopyroxene, and their minerals are closely packed ; Group II ones in contrast have black clinopyroxene, and their minerals are usually coarse and loosely packed. Intermediate ones are, however, found very frequently, having intermediate-colored (dull green) clinopyroxene. Dunite and clinopyroxenie of Group I are predominant over other rock species as xenoliths both in number and size in Takashima.

3.2.1 Group I

Group I xenoliths are dunite, wehrlite, clinopyroxenites, and websterites (Fig. 7). Olivine to clinopyroxene ratio is apparently gradual from dunite to clinopyroxenite. Clinopyroxene is predominant in volume over orthopyroxene in Group I pyroxenites. Rocks of Group I frequently exhibit layered or banded structures.

Dunite and wehrlite are medium-grained and have mosaic-equigranular texture (Plate

Table 1. Bulk rock chemistry of host alkali basalts of Kurose and Takashima. Cr_2O_3* & NiO*, numbers in parentheses are in ppm of Cr and Ni, respectively. Conventional wet chemical analysis by H. Haramura, University of Tokyo. KRh-1, vesicular basalt ; T-119, pale gray basalt ; T-058, gray basalt ; T-066, black basalt.

Locality	Kurose	Takashima		
No.	KRh-1	T-119	T-058	T-066
SiO_2	46.99	48.55	48.84	48.16
TiO_2	2.64	1.83	1.89	1.88
Al_2O_3	15.20	17.12	16.32	16.42
Cr_2O_3*	0.02	(280)	(192)	(288)
Fe_2O_3	3.04	4.83	3.42	2.62
FeO	7.90	4.95	6.44	7.62
NiO*	0.02	(206)	(128)	(152)
MnO	0.17	0.16	0.16	0.16
MgO	7.24	7.33	7.26	7.95
CaO	8.72	8.28	8.35	8.19
Na_2O	4.57	3.47	4.62	3.23
K_2O	1.03	1.89	1.87	1.83
P_2O_5	0.75	0.43	0.48	0.43
$H_2O(+)$	1.35	0.69	0.57	1.24
$H_2O(-)$	0.23	0.30	0.17	0.20
Total	99.91	99.81	100.39	99.98
Q	0.0	0.0	0.0	0.0
or	6.1	11.1	11.1	10.6
ab	27.6	29.4	24.7	26.7
an	17.9	25.6	18.1	25.0
ne	6.0	0.0	8.0	0.3
di	16.5	10.1	16.5	10.3
ol	13.0	11.3	11.8	17.3
mt	4.4	6.9	4.9	3.7
il	5.1	3.5	3.6	3.6
ap	1.8	1.0	1.0	1.0

III). Olivine exhibits kink band and wavy extinction, and pyroxenes scarcely have exsolution lamellae. Chromian spinel, usually associated with clinoyroxene, is brown to opaque in thin section, and varies from 0.2 to 7.7 % in volume. Orthopyroxene is rounded and included in clinopyroxene in wehrlite.

Clinopyroxenites are composed of clinopyoxene with subordinate amounts of olivine, chromian spinel and orthopyroxene. Clinopyroxene is mosaic and shows wavy extinction. Exsolution lamellae in clinopyroxene are not so abundant but is slightly more prominent than in dunite-wehrlite. Olivine is smaller in size than clinopyroxene, and is rounded in shape but is mosaic in olivine-rich parts. Orthopyroxene is various in shape, being coarse-grained and poikilitically enclosing olivine or being rounded and enclosed by clinopyroxene. Chromian spinel is opaque in thin section.

Websterites are composed of mosaic pyroxenes with exolution lamellae and wavy extinction. Orthopyroxene is sometimes kinked. Olivine is rounded and is also kinked. Chromian spinel is brown to opaque in thin section.

3.2.2 Lherzolite

One lherzolite xenolith of Group I (TKS-10) was found from Takashima (Arai and Kobayashi, 1984). It has protogranular to slightly porphyroclastic texture, and has olivine (70 %), orthopyroxene (20 %), clinopyroxene (8 %), spinel (0.2 %), sulfides (0.4 %) and others (1 %). Olivine and pyroxenes characteristically have numerous minute inclusion trails. Calcite is frequently found associated with clay minerals, and usually fills cracks or interstices of primary silicates, indicating secondary origin. It also occurs as rounded or bleb-like inclusions in fresh pyroxenes (Arai and Kobayashi, 1984). Sulfides (pyrite, pyrrhotite and pentlandite) are also found as composite grains.

3.2.3 Chromitite

Fine-grained chromitite of Group I is occasionally found as thin layers or streaks in dunitic rocks (Arai and Abe, 1994) (Plate III). Discrete xenoliths of chromitite are only rarely found : two of them were found to have so-called nodular texture (Plate III), which is characteristic of podiform (alpine-type) chromitite (Arai and Abe, 1994). They have rounded aggregates (nodules, up to 5 mm across) of fine-grained chromian spinel associated with pyroxenes, which are embedded in olivine-rich matrix.

3.2.4 Group II

Clinopyroxenites, websterites and orthopyroxenites mainly comprise Group II xenolith suite (Kobayashi and Arai, 1981 ; Fig. 7). They are mostly composed of coarse grains of pyroxenes that have spongy margins associated with fine-grained aggregates of plagioclase, olivine and spinel (Plate III). Pyroxenes have thick exsolution lamellae or blebs. Orthopyroxene sometimes shows wavy extinction. Olivine, rounded and sometimes kinked, is poikilitically enclosed by pyroxenes. Chromian spinel is rare and pyrrhotite is sometimes found. Coarse-grained gabbros of Group II are also found.

3.2.5 Orthopyroxene-rich veinlets (Group III)

Orthopyroxenite with or without plagioclase and clinopyroxene sometimes make veinlets in dunite and wehrlite xenoliths of Group I (Plate III). Discrete xenoliths of fine-grained orthopyroxenite that contain dunite fragments are not rare. They are equivalent to *Group III* xenoliths of Kobayashi and Arai (1981) and Arai and Kobayashi (1983). In these rocks replacement textures of olivine by orthopyroxene are clearly observed under the microscope. Plagioclase is found in central portions of relatively thick veins. Light-colored (greenish brown to grayish brown) aluminous spinel is occasionally found. Orthopyroxene is light purplish brown in thin section.

Kobayashi and Arai (1981) reported clinopyroxenite and websterites of Group III. They are mainly composed of coarse pyroxenes that have prominent exsolution lamellae, and green spinel. They are different from the orthopyroxenite mentioned above in grain size but is similar to each other in the abundance and color (light greenish to brownish) of spinel and the color of pyroxenes (light purplish brown) under the microscope (Kobayashi and Arai, 1981).

3.2.6 Composite xenoliths

Composite xenoliths (Irving, 1980) are very commonly found in Takashima. Dunite to clinopyroxenite of Group I is frequently enclosed or veined by black coarse-grained pyroxenite of Group II, indicating the younger generation of the latter. As mentioned above Group I dunite or wehrlite is sometimes veined by fine-grained orthopyroxenite (Group III).

Group II rocks are possibly younger than the fine-grained orthopyroxenite (Group III) because the latter appears to be invaded by Group II in the some composite xenolith (orthopyorxenite-veining dunite enclosed by Group II pyroxenite).

4. Mineral chemistry

Minerals were analyzed by electron microprobe (JEOL JXA-50 A) at Chemical Analysis Center of the University of Tsukuba when two of the authors (S.A. and H.H.) belonged to the University of Tsukuba. Additional microprobe (JEOL JXA-8800) analysis was done at the Center for Cooperative Research of Kanazawa University. Selected analyses are listed in Tables 2 and 3. Ferrous and ferric irons in spinel were calculated assuming spinel stoichiometry.

4.1 Kurose

Mineral chemical compositions show narrow ranges in ordinary mantle peridotites (harzburgite and clinopyroxene-poor lherzolite) in accordance with their small modal variations (especially cpx/(opx + cpx) ratio). Pyroxene-rich lherzolites have more fertile mineral chemistry (Table 2).

Table 2. Selected microprobe analyses of minerals in mafic-ultramafic xenoliths from Kurose. opx, orthopyroxene ; cpx, clinopyroxene ; pl, plagioclase ; lam, lamella ; FeO*, total iron as FeO. nd, not determined. Mg#, Mg/(Mg + total Fe) atomic ratio of silicates, and $Mg/(Mg + Fe^{2+})$ atomic ratio for spinel. Cr#, Cr/(Cr + Al) atomic ratio. Ca, Mg & Fe*, respective catonic fractions to (Ca + Mg + total Fe) in pyroxenes. Cr, Al & Fe^{3+}, respective cationic fractions to $(Cr + Al + Fe^{3+})$ in spinel. Ca, Na & K, respective cationic fractions to (Ca + Na + K) in plagioclase.

Rock	harzburgie (KR 225)				harzburgite (KR 376)				dunite (KR 384)		px-rich lherzolite (KR 383)			
Mineral	olivine	opx	cpx	spinel	olivine	opx	cpx	spinel	olivine	spinel	olivine	opx	cpx	spinel
SiO_2	41.54	57.85	55.25	0.01	41.26	56.23	53.02	0.14	41.71	0.10	40.77	55.07	52.08	0.05
Al_2O_3	0.02	1.84	1.97	24.27	0.02	3.53	3.35	44.67	0.02	17.23	0.02	4.48	5.35	60.22
TiO_2	0.00	0.02	0.07	0.22	0.01	0.02	0.07	0.07	0.01	0.31	0.01	0.05	0.21	0.07
Cr_2O_3	0.12	0.48	0.75	44.60	0.03	0.52	0.68	25.11	0.01	52.85	0.03	0.24	0.35	6.62
FeO*	9.70	6.16	2.44	17.07	9.26	6.06	2.57	12.70	7.68	15.94	12.28	7.44	3.33	12.80
NiO	0.31	0.17	0.01	0.00	0.35	0.16	0.10	0.26	0.38	0.07	0.26	0.08	0.13	0.44
MnO	0.14	0.21	0.04	0.30	0.19	0.16	0.07	0.26	0.11	0.28	0.14	0.21	0.15	0.17
MgO	50.38	35.30	18.69	14.96	49.14	33.06	17.15	18.74	50.47	14.66	47.02	30.94	15.34	20.63
CaO	0.08	0.93	23.46	0.00	0.07	0.92	21.29	0.01	0.10	0.03	0.08	0.77	21.96	0.00
Na_2O	0.01	0.03	0.30	nd	0.00	0.03	0.16	0.00	0.00	0.00	0.00	0.06	0.64	0.00
K_2O	0.00	0.00	0.00	nd	0.00	0.00	0.01	0.00	0.00	0.00	0.00	0.01	0.01	0.00
Total	102.22	102.96	102.99	101.87	100.33	100.68	98.44	101.94	100.48	101.45	100.59	99.31	99.50	100.99
Mg#	0.902	0.911	0.932	0.662	0.904	0.907	0.922	0.759	0.921	0.671	0.872	0.881	0.892	0.789
Cr#				0.548				0.274		0.673				0.069
Ca		0.017	0.457			0.018	0.451					0.015	0.479	
Mg		0.895	0.506			0.891	0.506					0.868	0.465	
Fe*		0.088	0.037			0.092	0.043					0.117	0.057	
Cr				0.524				0.267		0.646				0.066
Al				0.457				0.709		0.314				0.902
Fe^{3+}				0.037				0.024		0.041				0.032

Table 2. (continued)

Rock	sp-pl websterite (KR 22)				sp granulite (KR 320)				px granulite (KR 384)			Group II websterite (KR 381)				
Mineral	pl	opx	cpx	spinel	pl	opx	cpx	spinel	pl	opx	cpx	opx	opx lam	cpx	kars	rho
SiO_2	48.09	52.94	49.98	0.06	48.65	52.86	49.51	0.00	47.94	52.11	49.26	51.80	51.60	49.20	40.20	28.40
Al_2O_3	31.45	6.55	7.70	63.47	33.14	6.65	7.42	65.67	32.34	6.49	7.82	5.09	4.33	6.84	14.60	15.30
TiO_2	0.00	0.07	0.33	0.04	0.00	0.06	0.40	0.06	0.00	0.09	0.44	0.39	0.33	1.22	5.17	8.16
Cr_2O_3	0.00	0.05	0.10	1.85	0.00	0.09	0.08	1.53	0.00	0.10	0.17	0.09	0.11	0.12	nd	0.11
FeO*	0.27	11.36	5.15	16.36	0.17	10.16	4.41	14.18	0.11	12.31	5.68	15.80	15.70	8.57	10.00	21.40
NiO	0.00	0.08	0.01	0.23	0.00	0.04	0.09	0.27	0.00	0.07	0.00	nd	0.11	nd	0.14	nd
MnO	0.00	0.18	0.10	0.14	0.00	0.19	0.07	0.09	0.00	0.32	0.20	0.46	0.39	0.19	0.08	0.11
MgO	0.00	29.29	14.84	20.30	0.00	30.66	15.20	20.84	0.00	27.69	13.85	24.60	25.00	13.20	12.80	13.10
CaO	15.93	0.80	21.23	0.00	16.35	0.75	22.08	0.00	15.41	0.79	20.62	1.29	0.32	18.80	10.80	10.40
Na_2O	2.42	0.05	0.71	0.00	2.34	0.06	0.72	0.00	2.71	0.05	0.76	0.09	0.08	1.17	2.56	2.02
K_2O	0.12	0.00	0.00	0.00	0.06	0.00	0.00	0.00	0.08	0.00	0.00	nd	nd	nd	1.29	nd
Total	98.25	101.36	100.16	102.43	100.72	101.53	100.01	102.47	98.58	100.02	98.80	99.60	99.00	99.30	97.70	99.00
Mg#		0.821	0.837	0.758		0.843	0.860	0.770		0.800	0.813	0.736	0.739	0.733	0.872	0.640
Cr#				0.019				0.014								
Ca		0.016	0.463			0.015	0.473			0.016	0.465	0.027	0.027	0.428		
Mg		0.808	0.450			0.831	0.453			0.787	0.435	0.716	0.719	0.419		
Fe*		0.176	0.088			0.155	0.074			0.196	0.100	0.257	0.254	0.153		
Cr (Ca)	0.779			0.018	0.791			0.013	0.755							
Al (Na)	0.214			0.932	0.205			0.955	0.240							
Fe^{3+} (K)	0.007			0.050	0.004			0.032	0.004							

4.1.1 Group I and mafic granulite

Fo content and NiO content of olivine range from 89.9 to 91.2 (Fig. 8) and 0.3 to 0.4 wt%, respectively, in the mantle peridotite. Dunite has a slightly wider range of Fo content of olivine, from 88.8 to 92.3. Fo content of olivine is lower in pyroxne-rich lherzolite, being from 85.2 to 89.3.

The Mg# (= Mg/(Mg + total Fe) atomic ratio) of orthopyroxene ranges from 0.905 to 0.918, being slightly higher that of olivine in the mantle peridotite. Al_2O_3 , Cr_2O_3 and CaO contents range from 1.8 to 3.5 wt%, 0.5 to 0.6 wt % and 0.8 to 1.1 wt%, respectively. Olivine is very similar in composition between dunite and mantle peridotite, but Cr_2O_3 and CaO contents are slightly lower in the former. The Mg# of orthopyroxene ranges from 0.822 to 0.877 in pyroxene-rich lherzolite, from 0.788 to 0.848 in websterites and from 0.647 to 0.839 in mafic granulites. Al_2O_3 content of orthopyroxene varies from 4 to 5 wt%

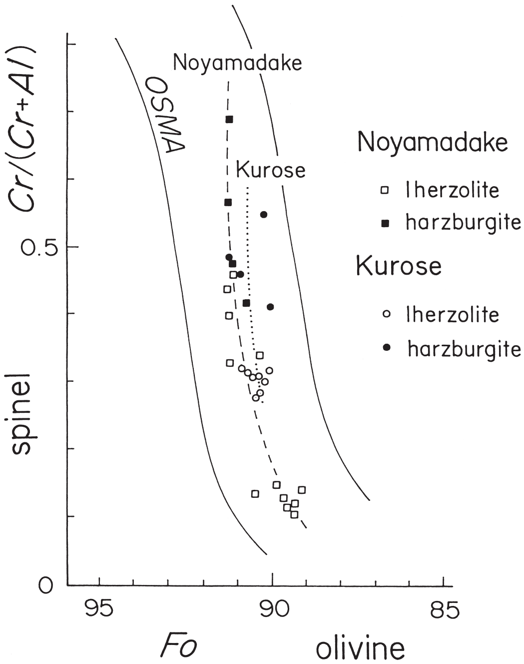

Fig. 8. Relationships between the Fo content of olivine and the Cr/(Cr+Al) atomic ratio of chromian spinel in peridotites from Kurose. Peridotites from Noyamadake (Fig. 1) are also plotted for comparison. Note that the Fo content of olivine is slightly lower at a given Cr# of spinel in Kurose than in Noyamadake. OSMA, olivine-spinel mantle array, a spinel peridotite restite trend by Arai (1994).

in pyroxene-rich lherzolite, from 4 to 7 wt% in websterite, and from 6 to 7 wt% in mafic granulite. Cr_2O_3 content of orthopyroxene ranges from 0.2 to 0.5 wt% in pyroxene-rich lherzolite, from 0.1 to 0.3 wt% in websterite, and from 0.1 to 0.2 wt% in mafic granulite.

The Mg# of clinopyroxene ranges from 0.911 to 0.932, which is slightly higher than that of coexisting olivine and orthopyroxene in mantle peridotite. Al_2O_3 and Cr_2O_3 contents of clinopyroxene in mantle peridotite range from 1.9 to 3.6 wt% and from 0.6 to 0.8 wt%, respectively. Clinopyroxene is relatively low in TiO_2 (less than 0.2 wt%) and in Na_2O (less than 0.5 wt%). The Mg# of clinopyroxene ranges from 0.861 to 0.893 in pyroxene-rich lherzolite, from 0.788 to 0.867 in websterites and from 0.688 to 0.861 in mafic granulites. Al_2O_3 content of clinopyroxene varies from 5 to 6 wt% in pyroxene-rich lherzolite, from 5 to 8 wt% in websterite, and from 6 to 9 wt% in mafic granulite. Cr_2O_3 content of clinopyroxene ranges from 0.4 to 0.8 wt% in pyroxene-rich lherzolite, from 0.2 to 0.6 wt% in websterite, and from 0.1 to 0.3 wt% in mafic granulite.

Cr# (= Cr/(Cr + Al) atomic ratio) of spinel ranges from 0.27 to 0.55 in mantle peridotite, being relatively narrow in concordance with the relatively small variation of petrographical characteristics (especially cpx/(opx + cpx) ratio) (Figs. 6 and 8). TiO_2 content is lower than 0.2 wt%, and $Fe^{3+}/(Cr + Al + Fe^{3+})$ atomic ratio varies from 0.02 to 0.04. The Cr# of spinel ranges from 0.06 to 0.15 in pyroxene-rich lherzolite, and from 0.02 to 0.1 in websterite. The ratio of spinel is lower than 0.02 in mafic granulite.

Plagioclase is calcic and An content varies from 76 to 93 in mafic granulite.

4.1.2 Group II

The Mg# is 0.74 in orthopyroxene and is 0.73 in clinopyroxene in Group II, being considerably lower than in Group I (Table 2). Al_2O_3 content is 5.0 wt% in orthopyroxene and is 6.8 wt% in clinopyroxene. Cr_2O_3 content is low (< 0.12 wt%) and Na_2O content is high (1.2 wt%) in clinopyroxene. In contrast TiO_2 content is high both in orthopyroxene (0.3 wt%) and in clinopyroxene (1.2 wt%). Kaersutite has about 5 wt% of TiO_2 and Mg# of 0.69. Rhoenite contains about 25 mole % of aenigmatite component and is slightly deficient in Ti (about 0.82 per formula unit).

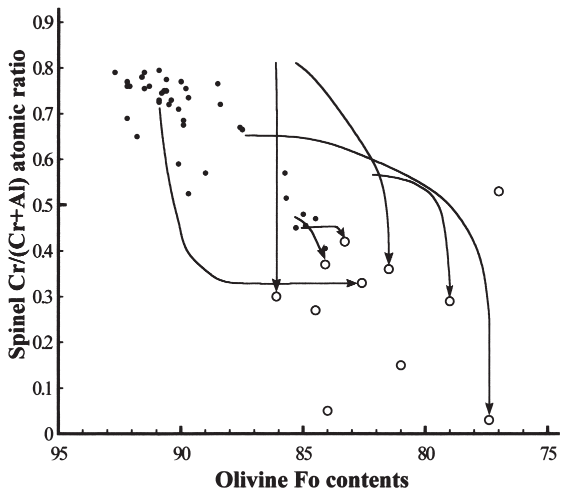

Fig. 9. Relationships between the Fo content of olivine and the Cr/(Cr+Al) atomic ratio of chromian spinel in dunite from Takashima. Solid circle, discrete dunite ; open circle, dunite clast in Group II or Group III. Solid curves with arrow indicate variations within the dunite clasts.

4.2 Takashima

4.2.1 Group I

Fo content of olivine in dunite is highly variable from 93 to 84 even for discrete xenoliths (Fig. 9). NiO content of olivine vary positively with the Fo content, while MnO content has a negative correlation. In composite xenoliths with pyroxenites of Group II or Group III, olivine in dunite parts regularly become Fe-rich toward the boundary (Fig.9). The variation is relatively sharp toward the dunite-Group III contanct and gradual toward the dunite-Group II contact. The Fo content of olivine appears to be bimodally distributed, around 90 and 85. As mentioned below, the Cr# of spinel varies in antipathy with the Fo of olivine (Fig. 9). Wehrlite and olivine clinopyroxenite have olivine of $Fo_{85.5\text{-}87.6}$ and $Fo_{84.7}$, respectively.

Chromian spinel in dunite demonstrates a wide range of composition ; the Cr# varies from 0.4 to 0.8 in discrete dunite xenoliths (Fig. 9). The Cr# of spinel becomes much lower in metasomatized dunite (Fig. 9). In individual samples coarser-grained spinels tend to be higher in Cr# than finer-grained ones. Chromian spinel in wehrlite and pyroxenites of Group I is lower in Cr# on average, < 0.6. Chromain spinel in Group I dunite exhibits large compositional variations when it is in contact with Group III pyroxenites. TiO_2 content of chromian spinel in dunite is usually lower than 2 wt% ; being < 0.5 wt% if coexisting with olivine of >Fo_{87} and > 0.8 wt% if coexisting with olivine of <Fo_{86}.

Chemical compositions of clinopyroxene significantly change depending on the lithological variation of Group I rocks. The Mg# varies from 0.93 in dunite to 0.83 in clinopyroxenite, and is most frequently 0.88 to 0.89. The ratio is generally higher than in

Table 3. Selected microprobe analyses of minerals in ultramafic xenoliths from Takashima. dun, dunite ; ol, olivine ; cpx'nite, clinopyroxenite ; opx'nite, orthopyroxenite ; mc, megacryst. Other abbreviations are the same as those in Table 2.

Rock	lherzolite (TKS-10)				dun (T-026)		dunite (T-078)			ol clinopyroxenite (T-036)				ol websterite (T-001)			
Mineral	olivine	opx	cpx	spinel	olivine	spinel	olivine	opx	spinel	olivine	cpx	opx lam	spinel	opx	cpx	spinel	olivine
SiO_2	40.30	54.70	51.60	nd	40.46	nd	40.51	55.86	nd	40.39	53.50	55.44	nd	53.00	50.90	0.11	nd
Al_2O_3	0.01	3.74	5.17	49.30	nd	9.93	0.00	3.20	26.66	0.03	2.86	2.40	23.61	3.48	4.54	31.30	42.11
TiO_2	0.00	0.05	0.34	0.48	nd	0.45	0.01	0.17	1.18	0.00	0.25	0.13	0.69	0.11	0.33	0.69	0.37
Cr_2O_3	0.00	0.26	0.29	10.80	0.06	52.61	0.06	0.28	29.08	0.02	0.71	0.48	34.89	0.33	0.60	28.60	16.55
FeO*	15.20	9.90	4.21	23.30	8.80	21.69	16.17	10.46	30.39	14.56	3.61	7.14	27.24	9.45	5.40	23.20	23.46
NiO	0.18	0.01	0.00	0.09	0.27	nd	0.17	0.11	nd	0.24	0.00	0.01	nd	0.05	0.02	0.20	nd
MnO	0.20	0.17	0.18	0.09	nd	0.26	0.27	0.30	0.25	0.26	0.22	0.26	0.37	0.23	0.25	0.14	0.21
MgO	45.50	30.30	15.80	15.30	49.24	12.15	44.89	30.79	12.04	44.57	16.94	32.17	11.83	30.20	16.90	14.00	16.02
CaO	0.14	1.02	22.70	nd	0.12	nd	0.16	1.03	nd	0.10	22.42	1.06	nd	1.53	18.90	0.06	nd
Na_2O	0.00	0.09	0.37	0.03	nd	nd	nd	nd	nd	nd	0.27	nd	nd	0.10	0.61	nd	nd
K_2O	0.00	0.00	0.00	0.00	nd	nd	nd	nd	nd	nd	0.00	nd	nd	0.00	0.00	nd	nd
Total	101.50	100.20	100.70	99.40	98.95	97.18	102.25	102.21	99.61	100.17	100.77	99.10	98.63	98.49	98.41	98.33	98.70
Mg#	0.850	0.845	0.870	0.631	0.909	0.611	0.832	0.840	0.561	0.845	0.893	0.889	0.558	0.851	0.848	0.519	0.675
Cr#				0.548		0.780			0.423				0.498			0.380	
Ca		0.020	0.474					0.020			0.459	0.021		0.030	0.406		
Mg		0.828	0.458					0.823			0.483	0.871		0.825	0.503		
Fe*		0.152	0.068					0.157			0.058	0.108		0.145	0.091		
Cr				0.118		0.702			0.359				0.436			0.340	
Al				0.800		0.198			0.491				0.440			0.554	
Fe^{3+}				0.082		0.100			0.150				0.123			0.106	

Table 3. (continued)

Rock	cpx'nite (T-025)		opx'nite (TK-003)		dunite I + websterite III (T-053b)					websterite III (T-201)			mc (TK-036)	mc (TK-054)
					dunite		websterite							
Mineral	cpx	opx	olivine	opx	olivine	spinel	opx	cpx	spinel	opx	cpx	spinel	cpx	opx
SiO_2	51.00	53.50	39.31	54.09	38.98	nd	52.12	47.79	nd	52.30	47.90	nd	47.43	52.23
Al_2O_3	6.17	5.14	0.03	3.42	0.00	18.52	5.56	8.59	52.87	6.29	8.18	56.70	9.15	5.72
TiO_2	0.76	0.30	0.00	0.23	0.02	0.82	0.28	1.14	0.80	0.36	1.28	0.52	1.50	0.29
Cr_2O_3	0.43	0.16	0.03	0.27	0.03	23.55	0.27	0.12	0.57	0.02	0.07	0.85	0.04	0.04
FeO*	6.35	12.70	15.58	9.55	21.47	48.54	13.61	8.16	30.15	12.90	7.16	25.80	9.02	12.23
NiO	0.00	0.08	0.35	0.03	0.27	nd	0.03	0.01	nd	0.01	0.12	nd	0.14	0.08
MnO	0.20	0.21	0.18	0.18	0.30	0.37	0.26	0.13	0.15	0.22	0.20	0.12	0.23	0.30
MgO	15.00	28.40	44.88	29.91	39.92	7.45	25.59	13.26	15.00	27.40	13.10	15.20	12.79	27.95
CaO	20.90	1.52	0.17	1.98	0.07	nd	1.51	18.89	nd	1.68	20.70	nd	17.85	1.18
Na_2O	0.63	0.09	nd	0.08	nd	nd	nd	0.66	nd	0.08	0.78	nd	0.99	0.09
K_2O	0.00	0.00	nd	0.00	nd	nd	nd	0.00	nd	0.00	0.00	nd	0.00	0.00
Total	101.40	102.04	10.53	99.74	101.05	99.24	99.24	98.76	98.66	101.51	99.43	99.29	99.10	100.09
Mg#	0.808	0.800	0.837	0.848	0.768	0.367	0.770	0.743	0.616	0.791	0.765	0.512	0.716	0.803
Cr#						0.460			0.007			0.010		
Ca	0.447	0.030		0.039			0.032	0.432		0.034	0.464		0.418	0.024
Mg	0.446	0.776		0.815			0.746	0.422		0.764	0.410		0.417	0.784
Fe*	0.106	0.194		0.146			0.222	0.146		0.202	0.126		0.165	0.192
Cr						0.307			0.006			0.009		
Al						0.360			0.859			0.897		
Fe^{3+}						0.333			0.135			0.094		

Groups II and III.

4.2.2 Lherzolite

The lherzolite (TKS-10) has iron-rich mineralogy (Arai and Kobayashi, 1984) (Table 3) : olivine is Fo_{85} in composition. The Cr# of chromian spinel is as low as 0.128, and Al_2O_3 and Cr_2O_3 in clinopyroxene are 3.74 wt% and 0.29 wt%, respectively. Carbonate is almost pure calcite.

4.2.3 Chromitite

Chromian spinel is highly chromiferous and its Cr# ranges from 0.6 to 0.8, which is equivalent to the range for typical podiform chromitites (Arai and Abe, 1994). The chromitite xenolith with nodular texture has especially high-Cr# spinel, the Cr# being around 0.8, which ratio is the same as that of the most typical podiform chromitite.

4.2.4 Group II

As is well known, minerals of Group II rocks are generally richer in Fe, Al and Ti than those of Group I (Fig. 10). Al_2O_3 and TiO_2 contents of clinopyroxene are 5 to 7 wt% and 1 to 1.8 wt%, respectively. Its Cr_2O_3 content is lower than 0.5 wt%. The Al_2O_3 content of orthopyroxene ranges from 3 to 5 wt%. The Mg# of pyroxenes ranges mostly from 0.80 to 0.85. Ca/(Mg + total Fe + Ca) atomic ratio of clinopyroxene is around 0.4.

4.2.5 Orhopyroxene-rich veinlets (Group III)

Rocks of Group III have relatively Fe-,Al-rich mineralogy except for thin veinlets within dunite. Al_2O_3 and TiO_2 contents of clinopyroxene are up to 9 wt% and > 1 wt%, respectively. The Al_2O_3 content of orthopyroxene ranges from 4 to 7 wt%. The Mg# of pyroxenes is lower than 0.8. Pyroxenes are usually lower in Mg# and are higher in Al_2O_3 and TiO_2 than those of Group II (Fig. 10). The Cr# of spinel is lower than 0.01. As mentioned above olivine and spinel in Group I dunite are modified to be Fe-richer and Al-richer, respectively, toward the contact with Group III pyroxenites. In accordande with this, pyroxenes and spinel in the Group III pyroxenites become magnesian and Cr-rich toward the contact with the dunite. In thin orthopyroxenite veinlests in dunite of Group I, orthopyroxene is high in Mg# (up to 0.89) and low in Al_2O_3 (2 wt%).

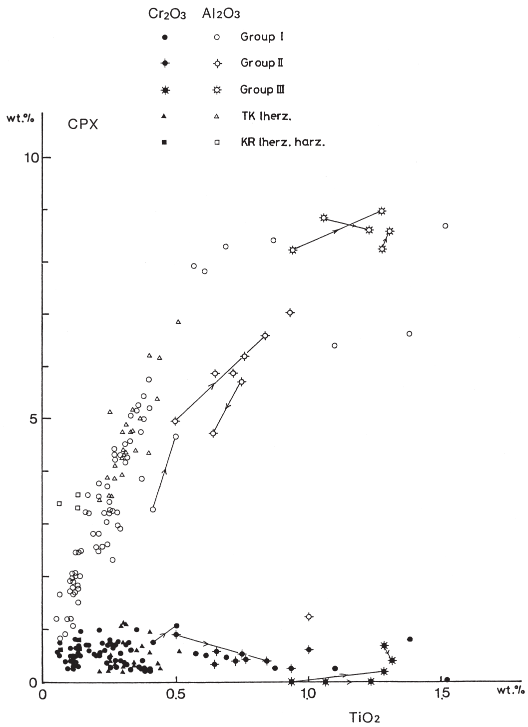

Fig.10. Relationships between the TiO_2 content and Cr_2O_3 and Al_2O_3 contents in clinopyroxene in ultramafic rocks from Takashima and Kurose.

4.2.6 Megacrysts

Megacrystal pyroxenes are similar in composition to equivalents in Group II pyroxenites (Arai et al., 2000). Plagioclase is mostly andesine (Aoki, 1970).

5. Geothermo-barometry

Equilibrium pressure can not be calculated because there are no good geobarometers for our rocks. All ultramafic rocks from Kurose and Takashima as the other xenoliths from Southwest Japan arc have neither olivine-garnet nor olivine-plagioclase assemblages, indicating they have been equilibrated within spinel lherzolite stability field (Fig. 11). Two-pyroxene temperatures are almost the same for the Kurose peridotites to mafic granulite, Group I and Group III rocks of Takashima. For example Wells' (1977) temperature is 1,000 to 1,100 ℃ for them all. Equilibrium temperature (Wells, 1977) for Group II rocks of Takashima is 100 ℃ higher, around 1,150 ℃ (Fig. 12).

The Kurose harzburgite/lherzolite has distinctly lower equilibrium temperature than, for example, Noyamadake lherzolite/harzburgite (Arai and Hirai, 1983 ; Hirai, 1986 ; Abe

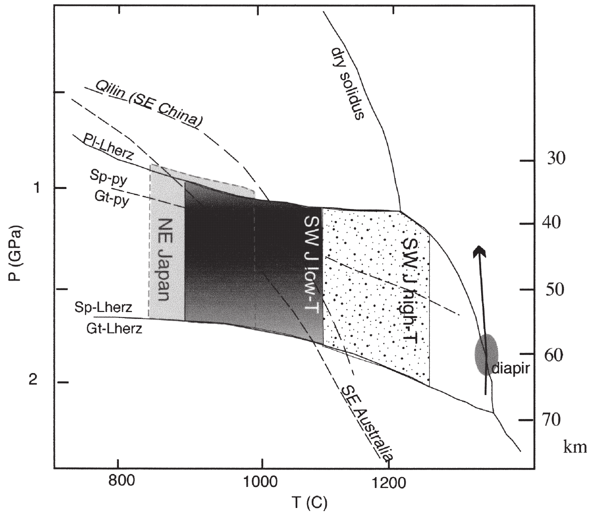

Fig.11. Pressure-temperature relationships of peridotite xenoliths from the Japan island arcs. The Kurose peridotite is within the region of " SWJ low-T". The temperatures are shown as histograms in Fig. 13. Geotherms of SE Australia and of Qilin (SE China) are after O'Reilly and Griffin (1985) and Xu et al. (1996), respectively. The phase boundaries are after O'Neil (1981), Takahashi and Kushiro (1983) and Gasparik (1987).

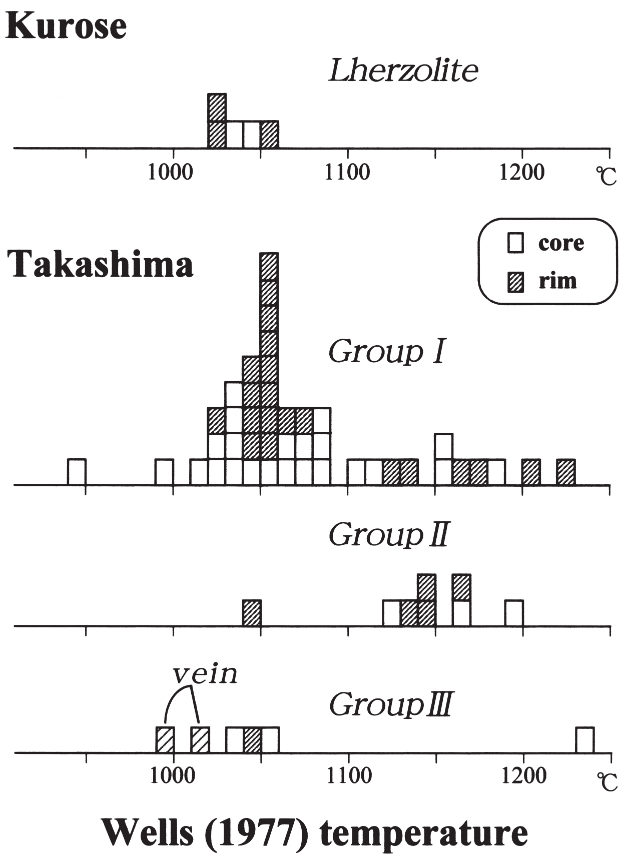

Fig. 12. Histograms of equilibrium temperatures (Wells, 1977) of Takashima and Kurose ultramafic xenoliths.

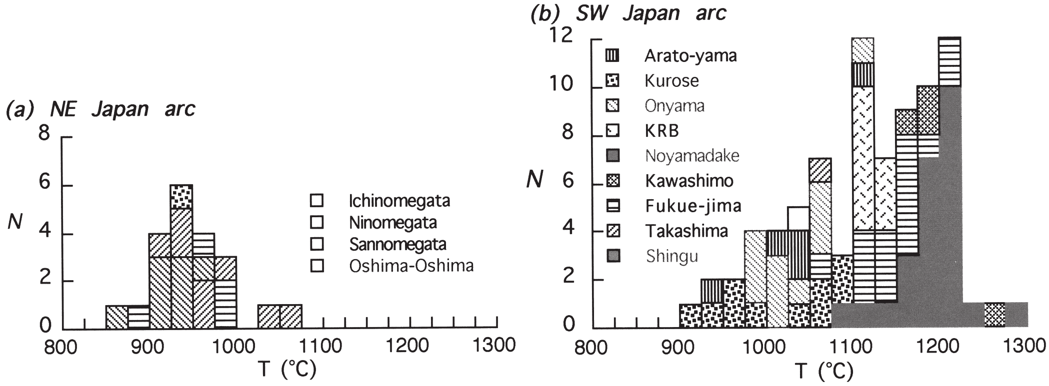

Fig.13. Equilibrium temperatures (Wells, 1977) of mantle peridotite xenoliths from the Japan island arcs. Note that the Kurose peridotite has relarively low temperatures. Data of Fukue-jima are from Umino and Yoshizawa (1996).

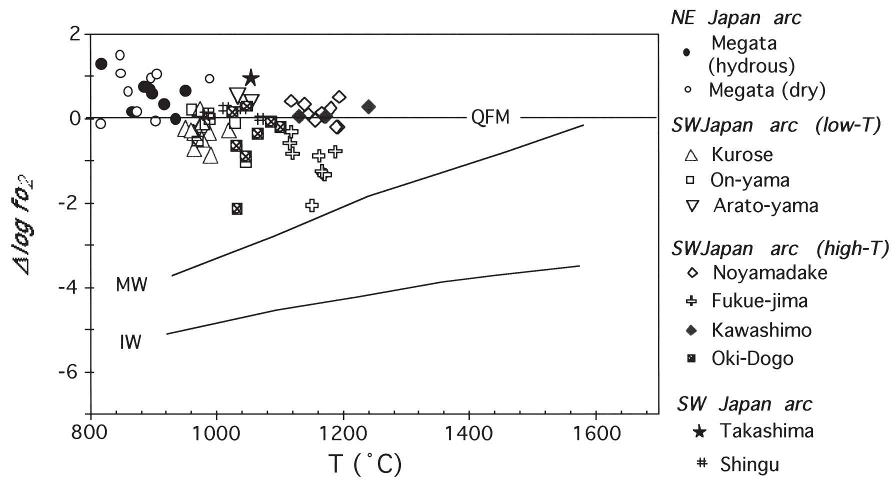

Fig.14. Relationships between the fO_2 and temperature of peridotite xenoliths from the Japan island arcs. Oxygen barometer by Ballhaus et al. (1991) and the thermometer by Sachtleben and Seck (1981). Note that peridotites from the Southwest Japan arc, including the Kurose peridotite, have low fO_2 than those from the Northeast Japan arc.

et al., 1999) (Fig. 13). Assuming a single geotherm, the upper mantle has a relatively high geotherm in the Southwest Japan arc (Abe and Arai, 2001), being higher than those of SE China (Xu et al., 1996) and SE Australia (O'Reilly and Griffin, 1985) (Fig. 11).

The fO_2 (Ballhaus et al., 1991) of the Kurose peridotite is slightly lower than that of QMF equilibration (Fig. 14). It is noteworthy that the fO_2 is higher in Megata peridotite xenoliths, which are sometimes hydrated, from the Northeast Japan arc than in peridotites, which are dry, from the Southwest Japan arc (Fig. 14).

6. Discussion

6.1 Origin of deep-seated rocks

6.1.1 Mantle peridotite

The Kurose peridotite is very similar in major-element chemistry to some abyssal peridotite. Na_2O content of clinopyroxene is relatively low (< 0.6 wt%) (Arai, 1991, 1994) and the Cr# of spinel is intermediate, from 0.3 to 0.5 (Arai, 1994) (Fig. 15). The Fo content of olivine is relatively low as compared at a given Cr# of coexisting spinel (Arai, 1994). The Kurose peridotite is a low-pressure mantle restite, formed either at mid-ocean ridge but now captured in arc regime or at in-situ island arc. This kind of peridotite is present at some part of sub-arc mantle ; possibly at the uppermost mantle of arc with thin crust.

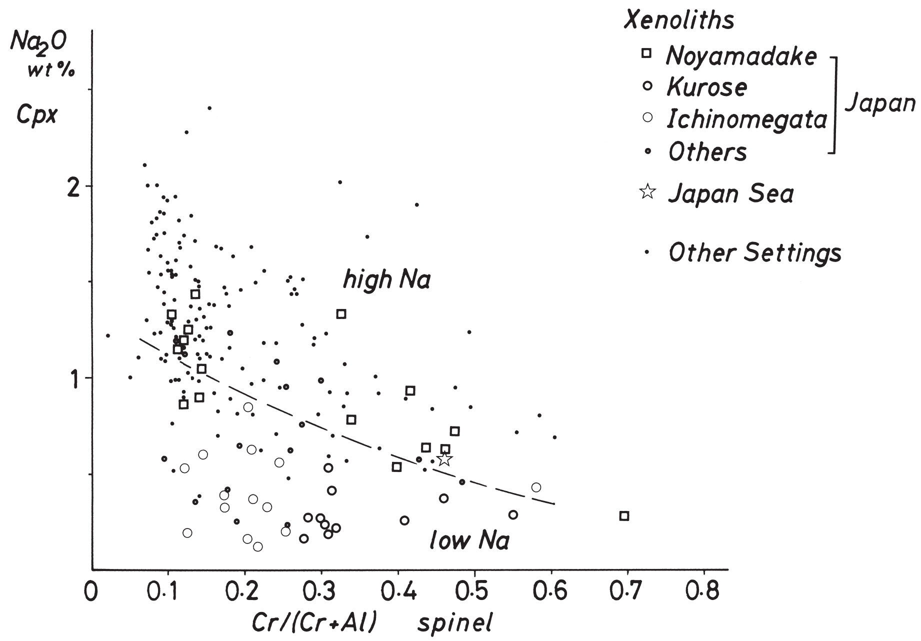

Fig.15. Relationships between the Na_2O content of clinopyroxene and the Cr/(Cr+Al) atomic ratio of chromian spinel in peridotite xenoliths. Note that the Kurose peridotite has relatively low Na_2O content of clinopyroxene.

Pyroxene-rich lherzolite and spinel websterites are possibly metamorphosed plagioclase-invaded peridotite and troctolite (or olivine gabbro), respectively (Fig. 16). This should be confirmed by trace-element geochemistry for clinopyroxene and bulk rock. Incompatibility of olivine with plagioclase in the Kurose xenoliths may support this interpretation.

6.1.2 Group I dunite-wehrlite-pyroxenites

Dunite, wehrlite and pyroxenites of Group I are basically cumulates, forming the ”cumulus mantle” of Takahashi (1978). Their mother magmas or magma may be of arc affin-

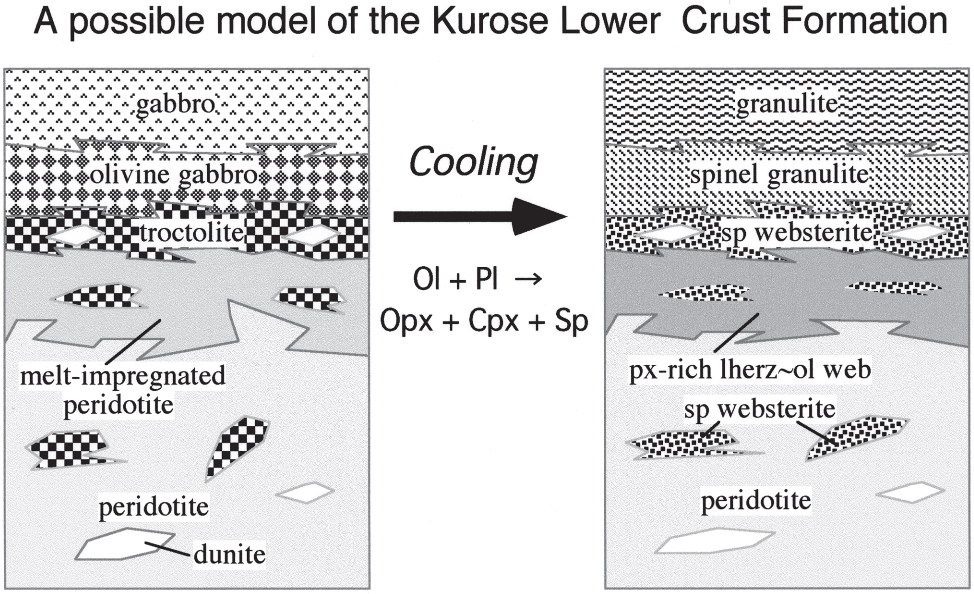

Fig.16. A possible model of the lower crustal rocks beneath Kurose deduced from xenoliths.

ity because of high Cr# (up to 0.8) and low Ti character of chromian spinel in most magnesian dunite (Fig. 9 ; Table 3). The wide range of Fo content of olivine in dunite (84 to 93) was possibly produced not by fractional crystallization but by metasomatism by the melt for Group II formation. It may be difficult to crystallize only olivine and spinel during the large variation of Mg# of melt upon fractional crystallization.

Possibly presence of podiform chromitite (Arai and Abe, 1994) associated with dunite suggests a peridotite/melt reaction origin for some dunite (see Arai and Yurimoto, 1994, 1995). The reactant peridotite is possibly similar to the Kurose harzburgite/lherzolite, which is approapriate to produce podiform chromitites (Arai, 1997). This further suggests that the Group I rocks partly form a kind of Moho transition zone (= dunite-dominant zone between lower harzburgite and upper layered gabbro of ophiolites) (Nicolas, 1989).

6.1.3 Group II pyroxenites and megacrysts

Clinopyroxenes of Group II pyroxenites are similar in chemistry to clinopyroxene megacrysts (Arai et al., 2000). As megacrsts have been considered to be high-pressure megacrysts of host alkaline basalts (Irving, 1974), Group II rocks are deep-seated cumulates from alkali basalts, which are akin to the host basalts but are slightly older in age. Their cognate origin can be denied because their pyroxenes have characteristics indicating deformation (kink bands) and subsolidus cooling (exsolution blebs and lamellae). This is consistent with the geologic situation of Takashima and Kurose alkali basalts mentioned above (Fig. 1). The Takashima alkali basalt belongs to the Higashi-Matsuura volcano clus-

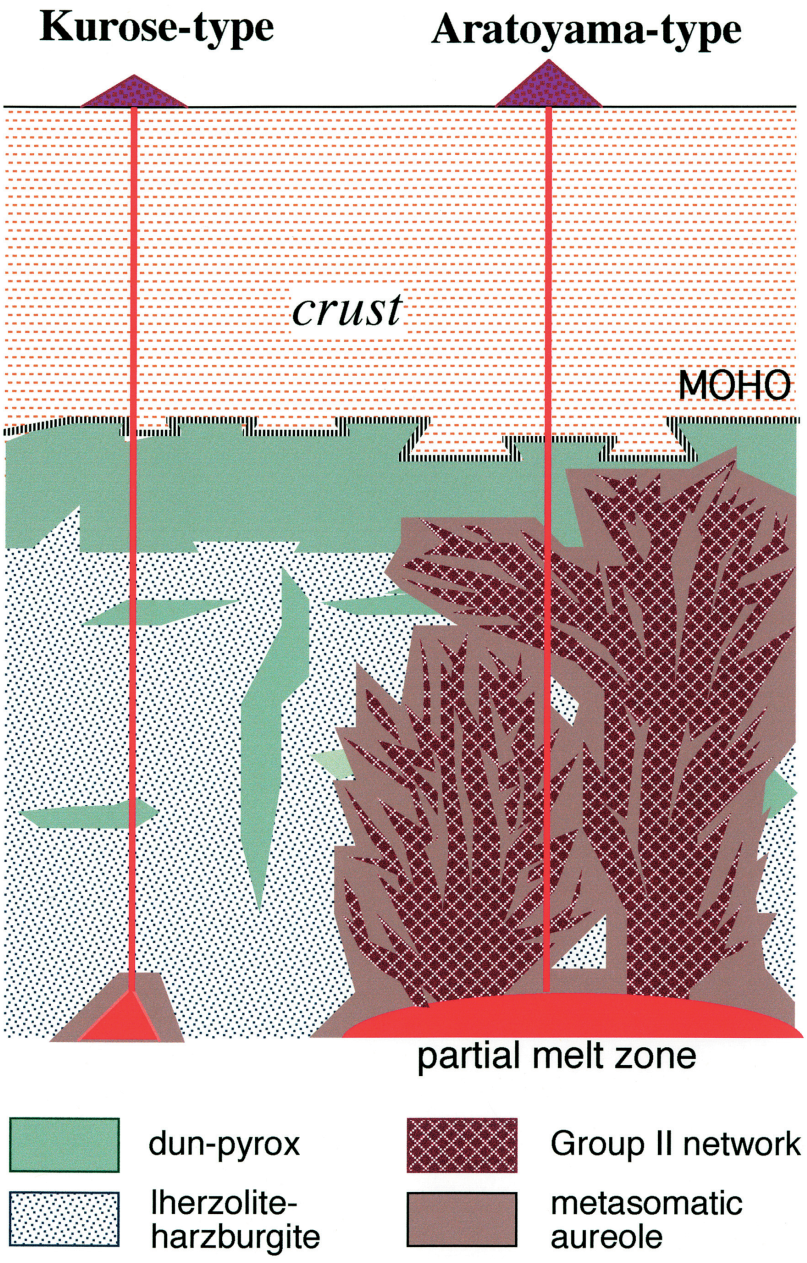

Fig.17. A petrological mode of the uppermost mantle beneath the Southwest Japan arc : two contrasting types. The Aratoyama-type mantle is characterized by invasion of dense network of Group II rocks within peridotite, and the Kurose-type one is almost free of Group II rocks. The fomer was developed beneath monogenetic volcano clusters, while the latter is representative of intact mantle beneath a solitary volcano (Fig. 1).

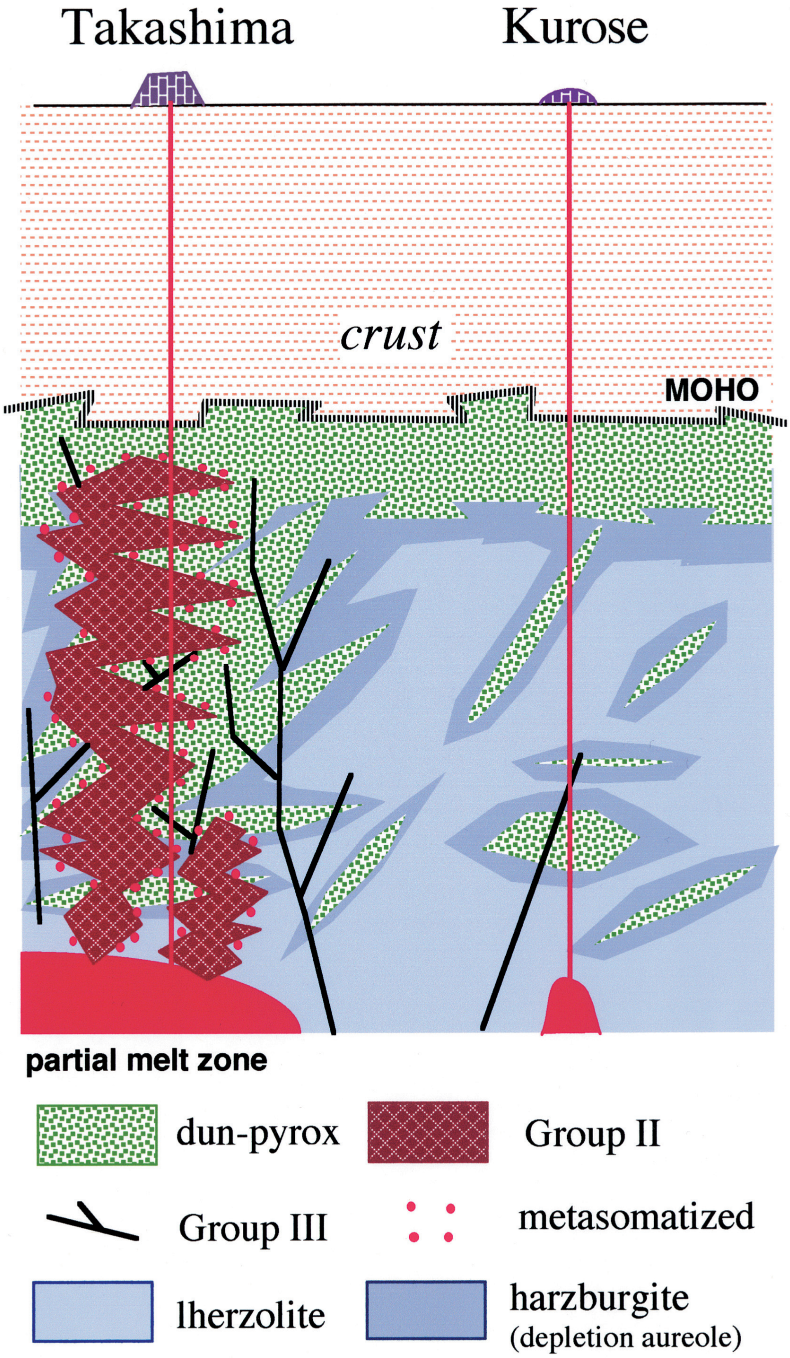

Fig.18. A petrological model of the uppermost mantle beneath northern Kyushu (Kurose-Takashima area). The mantle is strongly heterogeneous in terms of extent of Group II invasion, formation of dunite-pyroxenites of Group I.

ter, indicating that preceding activity of similar alkali basalt was highly possible in the upper mantle. On the contrary, the Kurose alkali basalt is solitary, and cumulates of Group II by consanguineous magma could not been produced. This is consistent with the scarcity of Group II xenoliths and black pyroxene megacrysts in the Kurose alkali basalt.

6.1.4 Group III

It is noteworthy that the melt for Group III rock formation was reactive with olivine to produce orthopyroxene. The pyroxenes are high in Fe, Ti and Al, and spinel is also highly aluminous. This strongly indicates an activity of Fe-,Ti-and Al-rich silica-oversaturated melt within the uppermost mantle (or Moho transition zone) of arc. We interpreted that the melt was derived from the then subducting slab.

6.2 Petrological heterogeneity of the upper mantle

Lateral heterogeneity of the upper mantle to lower crust is clearly shown by the difference of xenolith species between Kurose and Takashima, which are only 30 km apart (Arai et al., 2000).

6.2.1 Distribution of Group II rocks

Group II rocks and related megacrysts are almost absent in the Kurose xenolith suite. This indicates that the distribution of Group II rocks is highly heterogeneous laterally (Arai et al., 2000). The Kurose xenoliths are, therefore, devoid of metasomatism by the melt involved in Group II formation, and are expected to preserve their primary petrological characteristics (Arai et al., 2000). This kind of xenolith suite is very rare in the Southwest Japan arc, where monogenetic volcanoes of alkali basalts usually make clusters (Figs. 1 and 17).

The Group I rocks of Takashima, on the other hand, were possibly affected by the melt for Group II formation (Fig. 18), considering the large amount of Group II xenoliths associated with Group I xenoliths. It is possible that the negative corelationship between the Fo content of olivine and Cr# of chromian spinel in Group I dunite is partly a result of cryptic metasomatism by the melt for Group II formation. This may be suggested by the variation within dunite pieces captured by Group II pyroxenites (Kobayashi and Arai, 1981).

6.2.2 Distribution of Group I rocks

The possible ”Moho transition zone”, which is mainly composed of Group I rocks, is also changeable laterally (Fig. 18). The paucity of both lithological variety and relative volume of Group I dunite and pyroxenites in Kurose possibly means that dunite-wehrlite-pyroxenites of Group I characteristics are thin or small in volume relative to mantle peridotite beneath Kurose. The equilibrium temperature of Group I rocks from Takashima is similar to that of the mantle peridotite from Kurose, possibly indicating the similar depth of origin for the two xenolith suites. The thick cumulus mantle or Moho transition zone of arc origin may mean large activity of arc magma(s), leading to formation of a thick overlying arc crust.

7. Conclusions

The macmatic activites responsible for the formation of Group I dunite to pyroxenites and Group III rocks were related with arc magmas and slab-derived melts, respectively. Group II rocks and megacrysts are deep-seated cumulates and high-pressure phenocrysts of the preceding and present host alkali basalts, respectively. The alkali basalt magmatism was possibly related with opening of the Sea of Japan, a back-arc basin (Uto, 1990 ; Iwamori, 1991). They were derived from mantle diapers that were responsible for the Japan-Sea opening. The petrological lateral heterogeneity of the upper mantle deduced from the contrast between the two xenolith suites has been possibly made by continuous magmatic activities of arc and back arc settings of the Southwest Japan arc at the Western Pacific rim (Arai et al., 2000).

Acknowledgements

One of the authors (S.A.) greatly acknowledges Y. Kobayashi and M. Ikeda for their collaboration for Takashima and Kurose xenoliths, respectively. N. Nishida and K. Kadoshima helped us during the microprobe analysis. This is contribution no. 264 from the ARC National Key Centre for Geochemical Evolution and Metallogeny of Continents (www.es.mq.edu.au/GEMOC/).

References

Abe, N. and Arai, S. (2001). Comments on ”Garnet-bearing spinel harzburgite xenolith from Arato-yama alkali basalt, southwest Japan.” by Yamamoto et al. (1999). *Japan. Mag. Mineral. Petrol. Sci*., v.30, p.190-193.

----------,----------,and Yurimito, H. (1999). Texture-dependent geochemical variations of sub-arc mantle peridotite from Japan Island arcs. In *Proc. VIIth Intern. Kimberlite Conf*., J.B. Dawson Vol. (Gurney, J.J., Gurney, J.L., Pascoe, M.D., and Richardson, S.H., Eds.), p.1 3-22.

Aoki, K. (1970). Andesine megacryst in alkali basalts from Japan. *Contrib. Mineral. Petrol*., v.25, p.284 -288.

----------(1987). Japanese Island arc : xenoliths in alkali basalts, high-alumina basalts, and calc-alkaline andesites and dacites. In *Mantle Xenoliths* (Nixon, P.H., Ed.)., John Wiley & Sons, New York, pp.319-333.

----------and Shiba, I. (1973). Pyroxenes from lherzolite inclusions from Itinome-gata, Japan. *Lithos*, v.6, p.41-51.

----------and Prinz, M. (1974). Chromain spinels in lherzolite inclusions from Itinome-gata, Japan. *Contrib. Mineral. Petrol*., v.46, p.24 9-256.

----------(1987). Japanese Island arc : xenoliths in alkali basalts, high-alumina basalts, and calc-alkaline andesites and dacites. In *Mantle Xenoliths* (Nixon, P.H., Ed.)., John Wiley & Sons, New York, pp.319-333.

----------and Fujimaki, H. (1982). Petrology and geochemistry of calc-alkaline andesite of presumed upper mantle origin from Itinome-gata, Japan. *Am. Mineral*., v.67, p.1-13.

Arai, S. (1991). Petrological characteristics of the upper mantle peridotites beneath the Japan island arcs -Petrogenesis of spinel perid otites-.*Soviet Geology and Geophysics*, v.32, p.8-25.

----------(1994). Characterization of spinel peridotites by olivine-spinel compositional relationships : Review and interpretation. *Chem. Geol*., v.113, p.191-204.

----------(1997). Control of wall-rock composition on the formation of podiform chromitites as a result of magma/peridotite interaction. *Resource Geol*., v.47, p.177-187.

----------and Abe, N.(1994). Podiform chromitite in the arc mantle : chromitite xenoliths from the Takashima alkali basalt, Southwest Japan arc. *Mineral. Deposita*, v.29, p.434-438.

----------and Hirai, H. (1983). Petrographical notes on deep-seated and related rocks (1) Mantle peridotites from Kurose and Noyamadake alkali basalts, southwestern Japan. *Ann. Rep. Inst. Geosci. Univ. Tsukuba*, no.9, p.65-67.

----------,----------and Uto, K. (2000). Mantle peridotite xenoliths from the Southwest Japan arc : a model for the sub-arc upper mantle structure and composition of the Western Pacific rim. *Jour. Mineral. Petrol. Sci*., v.95, p.9-23.

----------and Kobayashi, K. (1981). Relative abundance of ultramafic rocks as inclusions in some alkali basalts from southwestern Japan and their bearing on the consititution of the upper mantle. *Ann. Rep. Inst. Geosci. Univ. Tsukuba*, no.7, p.66-69.

----------and----------(1984). Petrographical notes on deep-seated and related rocks (2) Carbonate-bearing iron-rich lherzolite xenolith in alkali basalt from Takashima, southwestern Japan. *Ann. Rep. Inst. Geosci. Univ. Tsukuba*, no.10, p.119-122.

----------and Yurimoto, H. (1994). Podiform chromitites of the Tari-Misaka ultramafic complex, southwestern Japan, as mantle-melt interaction products. *Econ. Geol*., v.89, p.1279-1288.

----------and----------(1995). Possible sub-arc origin of podiform chromitites. *The Island Arc*, v.4, p.104-111.

Ballhaus, C., Berry, R.F. and Green, D.H. (1991). High pressure experimental calibration of the olivine-orthopyroxene-spinel oxygen geobarometer : implications for the oxidation state of the upper mantle. *Contrib. Mineral. Petrol*., v.107, p.27-40.

Frey, F.A. and Prinz, M. (1978). Ultramafic inclusions from San Carlos, Arizona : petrologic and geochemical data bearing on their petrogenesis. *Earth Planet. Sci. Lett*., v.38, p.129-176.

Gasparik, T. (1987). Orthopyroxene thermobarometry in simple and complex systems. *Contrib. Mineral. Petrol*., v.96, p.357-370.

Hirai, H. (1983). Mode of occurrence of alkali basaltic volcanic products and their inclusions of Noyamadake, Shimane Prefecture, southwestern Japan. *Jour. Japan. Assoc. Mineral. Petrol. Econ. Geol*., v.78, p. 211-220 (in Japanese with English abstract).

----------(1986). *Petrology of ultramafic xenoliths from Noyamadake and Kurose, southwestern Japan*.

Unpub. D. Sc. Thesis, Univ. Tsukuba, 181 p.

Irving, A.J. (1974). Megacrsts from the Newer Basalts and other basaltic rocks of southeastern Australia. *Geol. Soc. Amer. Bull*., v.85, p. 1503-1514.

----------(1980). Petrology and geochemistry of composite ultramafic xenoliths in alkalic basalts and implications for magmatic processes within the mantle. *Am. Jour. Sci*., v.280-A, p.389-426.

Iwamori, H. (1991). Zonal structure of Cenozoic basalts related to mantle upwelling in southwest Japan. *Jour. Geophys. Res*., v.96, p.6157- 6170.

Katsui, Y., Yamamoto, M., Nemoto, S. and Niida, K. (1979). Genesis of calc-alkalic andesites from Oshima-Oshima and Itinomegata volcanoes, North Japan. *Jour. Fac. Sci. Hokkaido Univ*., v.19, p.157-168.

Kobayashi, Y. and Arai, S. (1981). Ultramafic nodules in alkali basalt from Taka-shima, Saga Prefecture, Japan. *Geosci. Rep. Shizuoka Univ*., v.6, p.11-24 (in Japanese with English abstract).

Kuno, H. (1964). Aluminian augite and bronzite in alkali olivine basalt from Taka sima, North Kyushu, Japan. In *Advancing Frontiers in Geology and Geophysics* (Subramaniam, H.P. and Balakrishna, E. Eds.), Indian Geophys. Union, Hyderabad, India, pp.205-220.

----------(1967). Mafic and ultramafic nodules from Itinome-gata, Japan. In *Ultramafic and Related Rocks* (Wyllie, P.J., Ed.), Wiley, New York, pp.337-342.

Mercier, J.C. and Noclas, A. (1975). Textures and fabrics of ultramaf ic peridotites as illustrated by xenoliths from basalts. *Jour. Petrol*., v.16, p.454-487.

Nakamura, E., McDougall, I. and Campbell, I.H. (1986). K-Ar ages fo basalts from the Higashi-Matsuura district, northwestern Kyushu, Japan and regional geochronology of the Cenozoic alkaline volcanic rocks in eastern Asia. *Geochem. Jour*., v.20, p.91-99.

Nicolas, A. (1989). *Structures of Ophiolites and Dynamics of Oceanic Lithosphere*. Kluwer, Dordrecht, 367 p.

Ninomiya, A. and Arai, S. (1992). Harzburgite fragment in a composite xenolith from an Oshima-Oshima andesite, the Northeast Japan arc. *Bull. Volcanol. Soc. Japan*, v.37, 269-273 (in Japanese).

Nixon, P.H. (Ed.) (1987). *Mantle Xenoliths*. John Wiley & Sons, New York, pp.384.

O'Neil, H.St.C. (1981). The transition between spinel lherzolite and garnet lherzolite, and its use as a geobarometer. *Contrib. Mineral. Petrol*., v.77, p.185-194.

O'Reilly, S.Y. and Griffin, W.L. (1985). A xenolith-derived geotherm for southeastern Australia and its geographical implications. *Techtonophysics*, v.111, p.41-63.

Sachtleben, T. and Seck, H.A. (1981). Chemical control of Al-solubility in orthopyroxene and its implications on pyroxene geothermometry. *Contrib. Mineral. Petrol*., v.78, p.157-165.

Sakuyama, M. and Koyaguchi, T. (1984). Magma mixing in mantle xenolith-bearing calc-alkalic ejecta, Ichinomegata volcano, northeastern Japan. *Jour. Volcanol. Geotherm. Res*., v.22, p.199-224.

Takahashi, E. (1978). Petrologic model of the crust and upper mantle of the Japanese island arcs. *Bull. Volcanol*., v.41, p.529-547.

----------(1986). Genesis of calc-alkaline andesite magma in a hydrous mantle-crust boundary : petrology of lherzolite xenoliths from the Ichinomegata crater, Oga Peninsula, Northeast Japan, part II. *Jour. Volcanol. Geotherm. Res*., v.29, p.355-395.

----------and Kushiro, I. (1983). Melting of a dry peridotite at high pressure and basalt magma genesis. *Am. Mineral*., v.68, p.859-879.

Takamura, H. (1973). Petrographical and petrochemical studies of the Cenozoic basaltic rocks on Chugoku Province. *Geol. Rep. Hiroshima Univ*., v.18, p.1-167.

Umino, S. and Yoshizawa, E. (1996). Petrology of ultramafic xenoliths from Kishyuku lava, Fukue-jima, Southwest Japan. *Contrib. Mineral. Petrol*., v.124, p.154-166.

Uto, K. (1990). *Neogene Volcanism of Southwest Japan : Its Time and Space on K-Ar Dating*. Ph.D. thesis, University of Tokyo, 184 p.

----------,Hirai, H., Goto, K. and Arai, S. (1987), K-Ar ages of carbonate-and mantle nodule-bearing lamprophyre dikes from Shingu, central Shikoku, Southwest Japan. *Geochem. Jour*., v.21, p.283-290.

----------,----------and Arai, S. (1993). K-Ar ages for Quaternary alkali basalts from Kurose, Fukuoka Prefecture and Kifune, Yamaguchi Prefecture, Southwest Japan. *Bull. Geol. Surv. Japan*, v.44, p.693-698 (in Japanese with English abstract).

Wells, P.R.A. (1977). Pyroxene thermometry in simple and complex systems. *Contrib. Mineral. Petrol*., v.62, p.129-139.

Xu, X., O'Reilly, S.Y., Zhou, X. and Griffin, W.L. (1996). A xenolith -drived geotherm and the crust-mantle boundary at Qilin, southeastern China. *Lithos*, v.38, p.41-62.

Yamamoto, M. (1984). Origin of calc-alkaline andesite from Oshima-Oshima volcano, north Japan. *Jour. Fac. Sci. Hokkaido Univ*., v.21, p.77- 131.

Plate I

Photomicrographs of typical peridotite xenoliths from the Japan island arcs. The scale is all the same (Scale bar, 0.5 mm). (a) to (c), from the Northeast Japan arc. (d) to (h), from the Southwest Japan arc. (a) Type I texture of Ichinomegata lherzolite (I-729). Textures of Types I, II and III are classified by Abe et al. (1999). Crossed-polarized light. (b) Depleted lherzolite with Type II texture from Ichinomegata (I-708). Note a large kinked olivine porphyroclast (upper). Crossed-polarized light. (c) Harzburgite with type III texture from Ninomegata (N-06) with strongly deformed texture. Crossed-polarized light. (d) Low-temperature type lherzolite from On-yama (ONY-127). The texture is slimiler to Type I of peridotite from Megata volcano. Note the small grain size compared with the Kurose peridotite. Crossed-polarized light. (e) High-temperature type lherzolite with protogranular texture from Noyamadake (OG-104). The texture is similar to the protogranular type of Mercier and Nicola (1975). Note the relatively large grain size and rounded pyroxenes with spongy rim. Plane-polarized light. (f) Weakly deformed lherzolite from Kawashimo (KWS-25) with protogranular texture similar to Noyamadake one. Crossed-polarized light. (g) Clinopyroxene-poor lherzolite (KWS-11) with porphyroclastic texture. Note the rounded form of pyroxene phorphyroclasts. Plane-polarized light. (h) The same as (g), with crossed-polarized light. Note the strong kink band in the olivine porphyroclast.

Plate II

Photomicrographs of mafic-ultramafic xenoliths from Kurose, the Southwest Japan arc. (a) Relatively fine-grained lherzolite (KR 120). Crossed-polarized light. (b) The same as (a). Plane-polarized light. (c) Harzburgite with porphyroclastic texture (KR 201). Note the absence of exsolution lamellae in orthopyroxene porphyroclast (left). Crossed-polarized light. (d) The same as (c). Plane-polarized light. (e) Spinel-rich olivine websterite to lherzolite (KR 383). Note the light color of spinel. Plane-polarized light. (f) Spinel websterite (KR 6). Note the dark green color of spinel. (g) Spinel-bearing granulite (KR 348). Note the symplectic aggregate of spinel and pyroxene. Plane-polarized light. (h) Websterite of Group II. Note the loose grain boundaries. Crossed-polarized light.

Plate III

Photomicrographs of ultramafic xenoliths and megacrysts from Takashima, the Southwest Japan arc. (a) Dunite of Group I (T-064). Crossed-polarized light. (b) Clinopyroxenite of Group II (T-179). (c) Dunite (Group I) with orthopyroxene-rich veinlet of Group III (center) (TK-3). Plane-polarized light. (d) The same as (c). Crossed-polarized light. (e) Orthopyroxene megacryst with fine-grained reaction rim (TK-40). Note the homogeneous appearance and the absence of exsolution lamellae. Crossed-polarized light. (f) Clinopyroxene megacryst (T-064). Note the homogeneous appearance and the absence of exsolution lamellae. Crossed-polarized light. (g) Fine-grained chromitite seam in dunite of Group I (T-037). Plane-polarized light. (h) Nodular-textured chromitite. Plane-polarized light.

Plate I

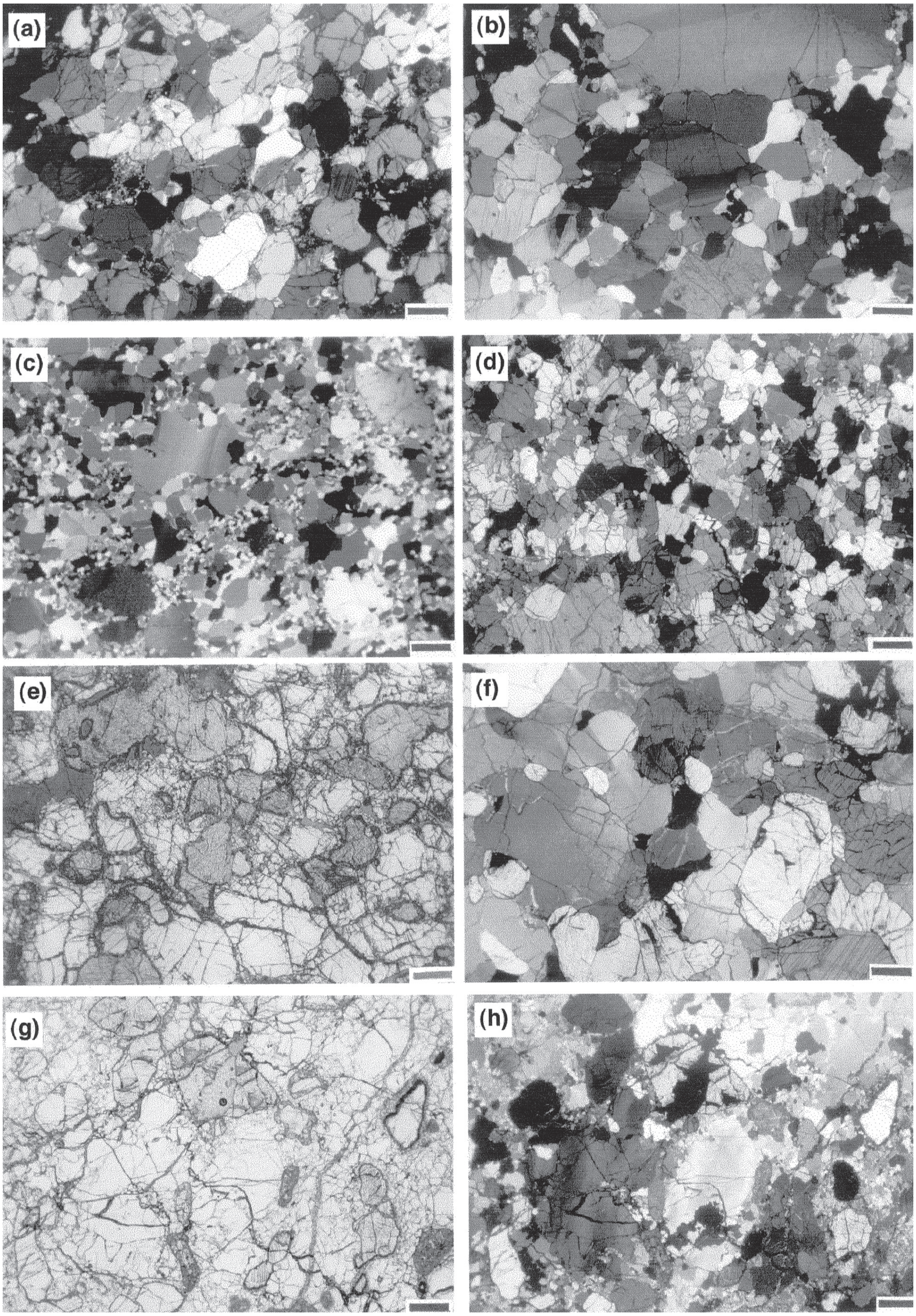

Plate II

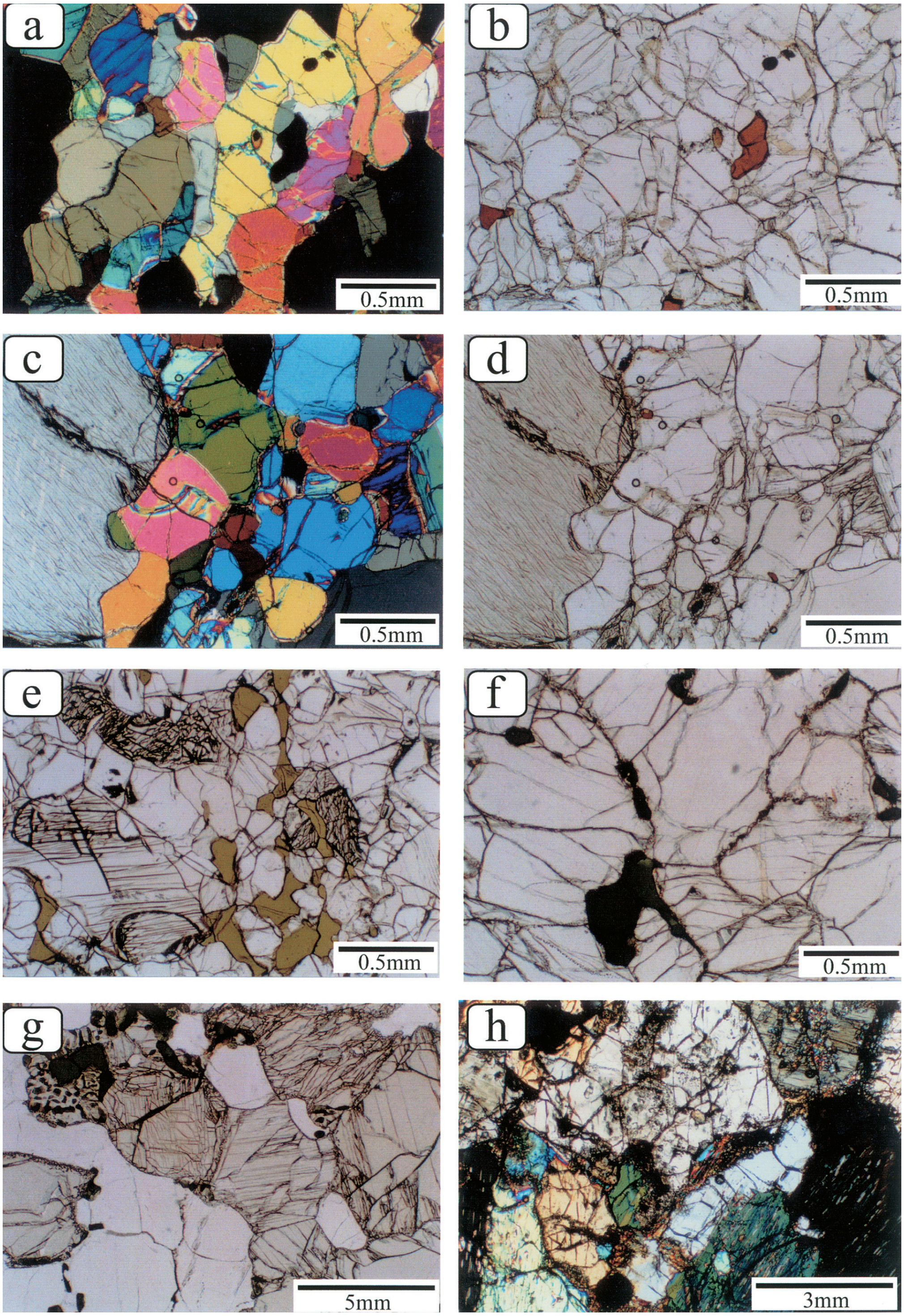

Plate III